NJC

RSC Publishing

PAPER

View Article Online
View Journal | View Issue

Cite this: *New J. Chem.*, 2013, **37**, 1046

Luminescent zinc salophen derivatives: cytotoxicity assessment and action mechanism studies†

Rosa Brissos,[a] David Ramos,[b] João Carlos Lima,[c] Francesco Yafteh Mihan,[d] Miquel Borràs,[b] Joaquin de Lapuente,*[b] Antonella Dalla Cort*[d] and Laura Rodríguez*[a]

Received (in Montpellier, France) 1st August 2012,
Accepted 16th January 2013

DOI: 10.1039/c3nj41125g

www.rsc.org/njc

The biological activity of two fluorescent Zn(II)–salophen derivatives has been evaluated. *In vitro* studies (AFM, emission and UV-vis titration with ethidium bromide and cell growth inhibition) show different mechanisms of interaction with DNA. It has been observed that these compounds enter the cells. Comet assays (with cultured fibroblast cells) have revealed that cellular uptake occurs without damaging the DNA strands. Preliminary studies carried out with living cells have shown IC_{50} values in a millimolar range, indicative of a non-cytotoxic behaviour. This fact could be understood by confocal microscopy co-localization studies with living cell internalization that have shown that, in fact, the compounds seem to enter the cells but not the nucleus under *in vivo* conditions.

1. Introduction

Real-time tracking of (bio-)molecules is a highly valuable tool to investigate cellular processes that implicate molecular motions.[1,2] Hence, molecular imaging can provide fundamental information regarding dynamic biological processes in living systems.[3–5] In this context, the breakthroughs achieved during the past five years in fluorescence microscopy,[6] thanks to the improvement of image resolution,[7,8] have boosted the emerging field of cell imaging, and generated remarkable advances in cell and molecular biology.[9,10] Accordingly, fluorescence probes have become some of the most powerful elements for molecular-imaging studies as a result of their high sensitivity and selectivity.[11–15]

Luminescent lanthanide-based compounds are the most prominent class of inorganic complexes used in bio-imaging.[16] However, transition-metal luminescent complexes, like zinc derivatives, are increasingly reported in the literature.[17]

Metal salen (salen: *N*,*N*′-bis(salicylidene)ethylenediamine) complexes are a long-standing, well-known family of coordination compounds that have found numerous applications in chemistry, depending on the nature of the metallic centre. Salen/salophen ligands (which act as planar tetradentate ligands with a *cis*-configuration around the metal ion) are capable of stabilizing various oxidation states of metal ions, hence controlling their performance in a large variety of useful catalytic transformations.[18–26] The redox properties of salen-containing coordination compounds have been used in biological studies in which their involvement in metal-dependent DNA-damage processes has been revealed.[27–35] For example, iron- and

[a] *Departament de Química Inorgànica, Universitat de Barcelona, Martí i Franquès 1-11, 08028 Barcelona, Spain. E-mail: laura.rodriguez@qi.ub.es; Fax: +34 934907725; Tel: +34 934039130*
[b] *Unitat de Toxicologia Experimental i Ecotoxicologia. Parc Científic de Barcelona, c/Baldiri i Reixach, 10-12, 08028 Barcelona, Spain. E-mail: jlapuente@pcb.ub.cat; Fax: +34 934037109; Tel: +34 934039710*
[c] *REQUIMTE. Departamento de Química, Faculdade de Ciências e Tecnologia, Universidade Nova de Lisboa, 2829-516 Monte de Caparica, Portugal*
[d] *Dipartimento di Chimica and IMC-CNR Sezione Meccanismi di Reazione, Università La Sapienza, Box 34 Roma 62, 00185 Roma, Italy. E-mail: Antonella.Dallacort@uniroma1.it; Fax: +39 06490421; Tel: +39 0649913087*

† Electronic supplementary information (ESI) available: AFM images of pBR322 plasmid DNA incubated with **1** for 24 h (Fig. S1); AFM images of pBR322 plasmid DNA incubated with **2** for 24 h (Fig. S2); electronic absorption spectra of complex **1** in the absence and presence of increasing amounts of ct-DNA. Inset: plot of [DNA] *vs.* [DNA]/($\varepsilon_a - \varepsilon_f$) (Fig. S3); emission spectra of ethidium bromide (EB) bound to DNA in the absence and presence of increasing amounts of **2**. Inset: Stern–Volmer plot: I_0/I *vs.* [**2**] (Fig. S4); normalized absorption spectra of **1** recorded at different pH values (Fig. S5); normalized absorption spectra of **2** recorded at different pH values (Fig. S6); microscopy images of 3T3 cells incubated for 24 h with concentrations of compound **2** above 70 μM. White light is used for co-localized cells. Green area represents fluorescent compound **2** (Fig. S7); 20× microscopy image of cells in DAPI-staining solution, using a UV2A fluorescence filter. Image of the negative effect on nucleotide in the presence of compound **2** (left) compared to positive control with MMS (right) (Fig. S8); binding-time studies of **1** with 3T3 cells. Pictures taken with a fluorescence microscope equipped with a UV2A filter (Fig. S9); binding-time studies of **2** with 3T3 cells. The pictures were taken with a fluorescence microscope equipped with a UV2A filter (Fig. S10); 20× fluorescence microscopy image of nucleoids incubated with **1** (concentration of 50 μg mL^{-1}) in the absence (left) and in the presence of 10% DAPI (right) (Fig. S11); fluorescence confocal microscopy image of 3T3 incubated cells with Draq5 (left), salophen complex **2** (middle) and superimposed images (right) (Fig. S12). See DOI: 10.1039/c3nj41125g

copper–salen derivatives may generate reactive oxygen species (ROS) in reducing environments, leading to oxidative DNA damage. For this reason they have been applied for drug–DNA foot-printing.[36] Recently, it has been shown that iron(III)–salophen (salophen = *N*,*N*′-bis(salicylidene)1,2-phenylenediamine) compounds can act as potent growth-supressing agents for ovarian-cancer cell lines *in vitro*, as well as a potential therapeutic drug for tumor treatment *in vivo*.[35,37] In addition, iron(III) complexes of salophen Schiff bases can undergo electron-transfer reactions mimicking the catalytic functions of peroxidases.[38] The formation of DNA adducts using Ni(II) complexes of redox-active ligands by covalent modification of nucleobases is also of great interest.[39] Some lanthanide–salophen complexes are able to bind neutral sugars and lipids, including lysophosphatidic acid that is a biomarker for several pathological conditions (like ovarian cancer).[40] A number of manganese–salophen and manganese–salen derivatives display cytoprotective features in fibroblast cultures *via* dihydrogen peroxide scavenging, and therefore are synthetic mimics of superoxide dismutase.[41,42] Very recent examples of new applications of salen derivatives haven been found such as liquid crystals, with a Mn(III) salen complex,[43] in the detection of Cu^{2+} in water and living cells with sulfonato–salen derivatives[44] and second order NLO properties.[45] Moreover, the possibility of salen/salophen derivatives to behave as excellent binders towards non-canonical DNA structures such as quadruplexes makes their use in this field very promising.[46–50]

Among such derivatives, the salen–salophen complexes of the non-redox metal ion zinc(II) are also quite important.[50–62] Their relevance is due to the fact that zinc is the second most abundant transition metal in living organisms after iron, and is the only metal which appears in all enzyme classes.[33] The molecular structure of these complexes features the metal centre in a five-coordinate square-pyramidal geometry with the ligand occupying the basal plane and a solvent molecule in the apical position. The closed-shell, d^{10} configuration of Zn(II) represents a key feature that can be exploited to design and produce ligand-dependent fluorescence materials[50,52,53] and luminescence chemosensors.[54–61] The lack of redox activity of Zn(II) normally generates Zn–salen compounds with low cytotoxicity.[53] So this, in addition to their potential intrinsic luminescence properties, makes them ideal candidates for the generation of biological fluorescence probes.[50,52,53]

In the study reported herein, the potential biological applications of two Zn(II)–salophen complexes, namely compounds **1** and **2**, are explored and their cytotoxicity is clearly assessed. Similar studies were performed also on the corresponding free ligands. To the best of our knowledge, this is the first investigation of this type regarding Zn(II)–salophen derivatives, while relevant work has been done instead with Zn–salen compounds (Chart 1).[63]

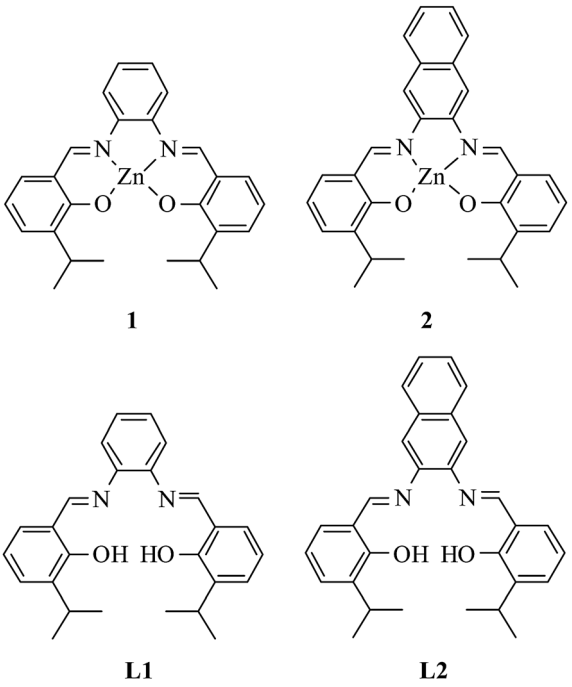

Chart 1

2. Experimental section

2.1. General

Compounds **1** and **2** have been synthesized as previously reported.[55] pBR322 plasmid DNA was obtained from Boehringer-Mannheim (Mannheim-Germany). HEPES (*N*-2-hydroxyethylpiperazine-*N*′-2-ethanesulfonic acid) was obtained from ICN (Madrid). 1,2-Diaminobenzene and 2,3-diaminonaphthalene were obtained from Aldrich. 3-Isopropylsalicylaldehyde was prepared from 2-isopropyl phenol (Aldrich) according to a general procedure.[64]

2.2. Physical measurements

The Atomic-Force Microscope (AFM) images were obtained with a nanoscope III multimode AFM system from Digital Instruments Inc. operating in tapping mode.

Fluorescence microscopy was carried out on an Olympus E800 equipped with a UV2A filter. The fluorescence emission spectra were carried out on a Horiba-Jobin-Yvon SPEX Nanolog-TM at 25 °C.

2.3. Synthesis and characterization

Synthesis of salophen-ligand L1. A solution of 3-isopropylsalicylaldehyde (0.355 g, 2.16 mmol) and 1,2-diaminobenzene (0.117 g, 1.08 mmol) in MeOH (2 mL) was stirred for 24 h at 60 °C. After some time an orange slurry precipitates from the cold solution. It was washed twice with cold MeOH and the final product was obtained as orange oil in 57% yield. ^{1}H NMR (200 MHz, $CDCl_3$) δ: 13.38 (s, 2H, OH), 8.64 (s, 2H, NH), 7.51–7.11 (m), 6.89 (t, J = 7.7 Hz, 2H, CH), 3.41 (hept, J = 6.9 Hz, 2H, CH), 1.26 (d, J = 6.9 Hz, 2H, CH_3) ppm. ^{13}C NMR (75 MHz, $CDCl_3$) δ: 164.33, 163.93, 159.16, 142.74, 136.86, 130.12, 127.64, 120.05, 118.77, 118.71, 26.79, 22.41, 22.11 ppm. HRMS-ESI-TOF for $C_{26}H_{29}N_2O_2^+$ calc.: 401.2229; found: 401.2250. Elemental analysis: calc. (%) for $C_{26}H_{28}N_2O_2$: C, 77.97; H, 7.05; N, 6.99%; found: C, 77.98; H, 7.06; N, 6.99%.

Synthesis of salophen-ligand L2. A solution of 3-isopropylsalicylaldehyde (0.208 g, 1.23 mmol) and 2,3-diaminonaphthalene (0.100 g, 0.632 mmol) in MeOH (3 mL) was stirred for 24 h. The mixture was then filtered and the final product was obtained as a pale yellow solid in 69% yield. ^{1}H NMR (300 MHz, $CDCl_3$) δ 13.38 (s, 2H, OH), 8.74 (s, 2H, NH), 7.86 (dd, J = 6.2, 3.3 Hz, 2H, CH), 7.49 (dd, J = 6.2, 3.2 Hz, 2H, CH), 7.40–7.19 (m, 6H, CH), 6.92 (t, J = 7.6 Hz, 2H, CH), 3.43 (hept, J = 7.0 Hz, 2H, CH), 1.27 (d, J = 6.9 Hz, 12H, CH_3) ppm. ^{13}C NMR (75 MHz, $CDCl_3$) δ: 164.42, 159.28, 143.02, 136.91, 132.86, 130.24 130.19, 127.82, 126.39, 118.85, 118.77, 116.89, 26.83, 22.42 ppm. HRMS-ESI-TOF for $[C_{30}H_{30}N_2O_2K]^+$ calc.: 489.1944; found: 489.1954. Elemental analysis: calc. (%) for $C_{30}H_{30}N_2O_2$: C, 79.97; H, 6.71; N, 6.22%; found: C, 79.98; H, 6.72; N, 6.22%.

2.4. Atomic-force microscopy experiments

pBR322 DNA was heated before use at 60 °C for 10 min to obtain the open circular (OC) form. Stock solution is 1 mg mL^{-1} in a buffer solution of HEPES. Each sample contains 1 μL of DNA pBR322 of concentration 0.25 μg μL^{-1} for a final volume of 50 μL. All the Stock solutions were freshly prepared before use in milli-Q water with 2% DMSO.

2.5. UV-vis spectrophotometric studies

The absorption titrations were performed by adding increasing amounts of ct-DNA DNA (calf thymus DNA) to the complexes in Tris–HCl buffer (5 mM) and NaCl (50 mM) at pH = 7.2. The concentration of ct-DNA was determined from the absorption intensity at 260 nm with a molar extinction coefficient of 6600 M^{-1} cm^{-1}. After addition of DNA to the metal complex, the resulting solution was allowed to equilibrate at 25 °C for 2 min, after which absorption spectra were recorded.

2.6. Fluorescence spectrophotometric titrations

The relative binding affinities of the complexes to ct-DNA were studied with an EB-bound (EB stands for ethidium bromide) ct-DNA solution in 5 mM Tris–HCl/50 mM NaCl buffer (pH = 7.2). The fluorescence spectra were recorded at room temperature with excitation at 514 nm. The titration experiments were carried out with an EB–DNA solution containing 2.5×10^{-5} M EB, 1×10^{-5} M ct-DNA and 75×10^{-3} μg μL^{-1} of the compounds.

2.7. Cytotoxicity studies

For the cytotoxicity assays, 3T3 Balb/c cells were cultured in Dulbecco's modified Eagle's medium (DMEM, Sigma-Aldrich) containing 10% fetal calf serum (Hyclone), 2 mM glutamine (Sigma-Aldrich) and antibiotics (Sigma-Aldrich, 50 μg mL^{-1} penicillin and 50 μg mL^{-1} streptomycin). Thus cells were incubated for 24 h for correct adhesion and then, decreasing solutions of the salophen compounds at 10% were applied in some wells together with a solvent control (sterile water at 10%) and a positive control (0.2% sodium dodecylsulfate, *i.e.* SDS, which is a known cytotoxic agent), and they were incubated for 24 h. The cells were exposed to a range of concentrations from 2155.73 to 8.43 μM for compound **1** and 1945.75 to 4.55 μM for compound **2**, both with a dilution of 2-fold each time for 24 h under 5% CO_2 at 37 °C. The viability was assessed by the MTT assay based on the mitochondrial dehydrogenase enzyme capability to hydrolyze chromogen bromide (3-(4,5-dimethylthiazol-2-yl)-2,5-diphenyltetrazolium bromide). The cells were washed with PBS (3×) and fresh medium was added together with a 5 mg mL^{-1} MTT solution and incubated for 2 h at 37 °C, under a 5% CO_2 atmosphere This compound shows a pale-yellow color in solution; by the action of enzymes, MTT is reduced to formazan in the mitochondria of living cells, a crystallized, dark blue compound that cannot cross the cell membrane.

A second cytotoxicity assay was carried out using DMSO as a solvent with the same concentrations of compounds that previously assayed. The maximum dose of DMSO and compounds used was 1%.

The data were statistically analyzed to calculate the 50% inhibition concentrations, IC_{50}, using the SPSS program, version 15 for Windows applying Probit Regression.

2.8. Genotoxicity-comet assay

The genotoxicity study on the 3T3 Balb/c fibroblast cell line was performed *via* the *Comet Assay* that was carried out according to the guideline ASTM-E2186.[65]

Cells were cultured in 6-well flat-bottom microtiter plates containing 2 mL of cell suspension (2×10^5 cells approximately). After 24 h of incubation at 37 °C with 5% CO_2, the compound to be investigated was added. Due the data obtained in cytotoxicity assay, only 2 doses were needed. For compound **1** we exposed 16.86, 8.43 μM and for compound **2**, 583, 71 and 291.86 μM with a solvent control with 1% DMSO. After 24 hours of exposition, the 3T3 fibroblast cells were detached from the well with 0.05% trypsin solution and collected by centrifugation. Cells were embedded in low-melting point 0.9% agarose (LMP-Gibco) prepared in MilliQ water (18 MΩ), and layered on pre-coated slides. The slides were placed in lysing buffer (2.5 M NaCl, 100 mM Na_2EDTA, 10 mM Tris pH 10, *N*-lauryl-sarcosine 1% (w/v) (Sigma)) with 1% Triton X-100 for 1 h at 4 °C. The isolated DNA of the nuclei in the agarose gels was unwinded for 40 min in electrophoresis buffer (1 mM Na_2EDTA and 300 mM NaOH, pH > 13). The SCGE slides were then electrophoresed for 30 min at 25 V and 300 mA, at 4 °C. After neutralization with 400 mM Tris buffer (pH 7.5), the slides were dried at room temperature. For image analysis, the slides were hydrated and stained with 10 μL of DAPI at 14.28 μM. Non-damaged cells exhibit a spherical shape, while fragmented nucleoids migrate, forming a tail (''comet'' shape). The nucleoid damage was quantified as fluorescence percentage in the tail. In the assay, the percentage of DNA in the tail was determined in respect to the intensity of the total DNA, in 50 cells. The determination was obtained with the software *Comet Assay IV* and the corresponding statistical using the SPSS program version 15 for Windows applying Mann–Whitney *U* statistics.

2.9. Preliminary cellular uptake studies

3T3 Balb/c cells were exposed to two different concentrations of compounds: **1** (4.31 and 8.62 μM) and **2** (3.89, 7.78 μM) both in DMSO and they were observed on an inverted fluorescence

microscope with two different filters (B2A and UV2A) co-stained with acridine orange and 4′,6-diamidino-2-phenylindole (DAPI). Observations were carried out at different times: 15, 30 minutes, 1 h, 1.5 h, 2 h and 24 h after exposition.

2.10. DNA binding studies in cells

Preliminary experiments were carried out with free nucleoids in an agarose matrix. Fixed nucleoids were stained with concentrations of compounds **1** and **2** of *ca.* (107.78 μM, 97.29 μM) (see comet assay protocol). Staining with DAPI (4′,6-diamidino-2-phenylindole, 14.28 μM), a well-known fluorescent stain that acts as a DNA minor-groove binder and DNA intercalator, at a concentration of 5 μg mL^{-1} allowed us to obtain better microscopy images.

For living internalization of compounds, 3T3 cells were seeded onto a cover slip in a 24-well plate and grown overnight under normal growth conditions followed by incubation of **1** at 28.02 μM or **2** at 97.29 μM for an additional 3 h. Control cells were treated with an equivalent amount of DMSO. Cells were fixed with 4% formaldehyde in PBS for 30 min, washed twice with PBS, and permeabilized with 0.2% Triton X-100 in PBS for 5 min. The cells were washed three times with cold PBS followed by incubation with Draq5 (10 μM) for 30 min at room temperature. Stained cells were washed three times with cold PBS, mounted on a microscope slide with mounting media Mowiol and visualized under a Leica TCS SP2 AOBS system (405 nm excitation laser diode for 2 molecules and 688 nm for Draq5). To detect molecules inside the cell, we performed a lambda scan with a wide range of wavelengths. With Z plain fixed inside the nucleus thanks to Draq5 co-localization stain, pictures were taken at different wavelengths, from 405 to 600. We selected different points of the cell and measured the intensity of the light emitted from each region.

3. Results and discussion

L1 and **L2** were prepared using the appropriately substituted salicylaldehyde and 1,2-diaminobenzene as starting materials. The reactants were stirred in methanol for 24 h and the products precipitated upon cooling the solution. The orange crystals were collected by vacuum filtration and washed with ice-cold methanol. Characterization by different spectroscopic techniques and mass spectrometry verifies the formation of the desired compounds. As stated above, the corresponding Zn derivatives **1** and **2** were prepared according to the literature.[55]

Fluorescence spectrophotometric measurements, previously reported by some of us, showed that **1** and **2** recognize anions of biological relevance, *i.e.* the nucleotides AMP^{2-}, ADP^{3-}, and ATP^{4-}.[56] The electronic absorption spectra of the complexes display broad unstructured bands in the 240–500 nm range.[55,56] Excitation at both low energy bands led to a broad emission band centred at 530 and 532 nm for **1** and **2** respectively.[56]

The risk of cytotoxic effects from exposure to Zn(II)-containing derivatives is lower (zinc is indeed an essential trace element)[50,52,53] when compared to other transition metals or lanthanides. Moreover, the luminescent properties displayed by **1** and **2** encouraged us to investigate their potential use as markers in cellular uptake processes. Obviously to do this the cytotoxic effects should be evaluated and compared with those of the corresponding metal-free ligands **L1** and **L2**.

DNA-binding processes and mechanisms have been firstly investigated by the interaction of **1** and **2** with isolated DNA using Atomic Force Microscopy (AFM) and UV-vis and fluorescence titration experiments.

3.1. AFM studies

Free pBR322 plasmid DNA was incubated for 5 h and 24 h with DMSO solutions of **1** and **2** and AFM images were taken subsequently (see Fig. 1, 2 and Fig. S1 and S2, ESI†). After an incubation time of 5 h with **1** (Fig. 1), the initial OC form of DNA disappears completely, giving rise to the formation of mixed toroidal and plectonemic supercoils, as well as to complete plectonemic supercoiling, most likely due to the intercalation of the complexes into the DNA molecules. In the case of **2**, the OC form of DNA is comparatively much less affected (Fig. 2) but plectonemic supercoiled regions are still observed (although sparsely), which again suggest intercalation of the salophen compound. After an incubation time of 24 h, the intercalating properties of both compounds are further corroborated, as a strong clustering of DNA is observed, producing rod-like aggregates (see Fig. S1 and S2, ESI†).

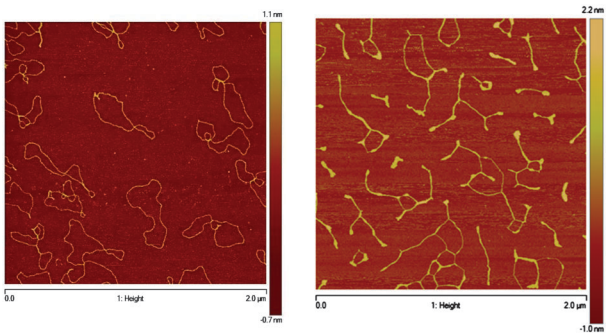

Fig. 1 AFM image of pBR322 plasmid DNA (left) and pBR322 plasmid DNA (0.10 μM) incubated with **1** (0.33 μM) for 5 h (right).

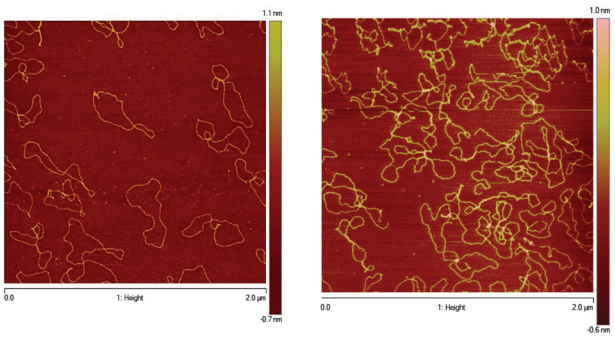

Fig. 2 AFM image of pBR322 plasmid DNA (left) and pBR322 plasmid DNA (0.10 μM) incubated with **2** (0.15 μM) for 5 h (right).

As mentioned above, Zn-based compounds are not expected to present cytotoxic properties. However with the perspective of using our derivatives as biomarkers, we decided to analyze their potential cytotoxicity (see Section 3.4).

3.2. DNA-binding studies by absorption and emission titrations

Absorption spectra of the complexes with increasing amounts of added DNA were recorded (Fig. 3 and Fig. S3, ESI†). A decrease in molar absorptivity (hypochromism) and slight bathochromism (2–5 nm) which is larger for **2**, probably due to the planarity of the naphthalene ring, is observed for the two complexes. Such variations are indicative of a likely intercalation mode of the two complexes into ct double helix DNA, most likely similar to that obtained with ethidium bromide, EB (see below).[66] Nevertheless, the association constant between DNA and ethidium bromide is two orders of magnitude higher than the one calculated for our complexes showing that EB is a stronger intercalating agent.

Binding affinity of the complexes with DNA, K_b, could be determined quantitatively by using the following equation:[67]

$$[\mathrm{DNA}]/(\varepsilon_a - \varepsilon_f) = [\mathrm{DNA}]/(\varepsilon_b - \varepsilon_f) + 1/K_b(\varepsilon_b - \varepsilon_f)$$

where [DNA] is the concentration of ct DNA in base pairs, ε_a, ε_f, and ε_b are the apparent extinction coefficient corresponding to A_{obs}/[complex], the extinction coefficient for the unbound compound and the extinction coefficient for the compound in the fully bound form, respectively.

The binding constants K_b for **1** and **2** were found to be 1.7×10^5 M^{-1} and 1.6×10^5 M^{-1} respectively, therefore suggesting a similar strength interaction of both complexes with DNA. These values are similar to those reported recently in the literature for DNA metallointercalators containing N-donor ligands (*e.g.* ethylenediamine, hydrazone).[68,69]

Further support for the binding of the complexes to DNA by intercalation mode was provided by competitive binding experiments with ethidium bromide (EB). This planar compound is non-emissive in phosphate buffer (pH 7.2), due to fluorescence quenching of free EB by solvent molecules, but emits intensely in the presence of DNA as a result of its intercalation between adjacent DNA base pairs. When a second species is added, this can compete with EB for DNA binding sites causing the decrease in the fluorescence intensity. The quenching is due to the reduction of the number of DNA binding sites available to the EB. Therefore EB is used as a common fluorescent probe for DNA structure able to provide information about the mode and the process of single species binding to DNA.[70]

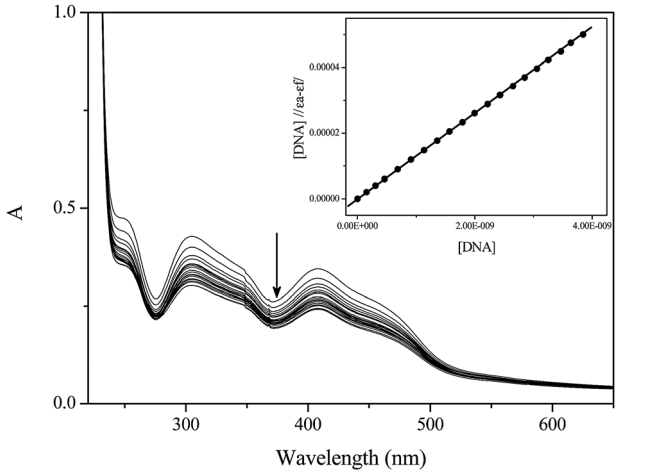

Fig. 3 Electronic absorption spectra of complex **1** in the absence and presence of increasing amounts of DNA. Inset: Plot of [DNA] *vs.* [DNA]/($\varepsilon_a - \varepsilon_f$).

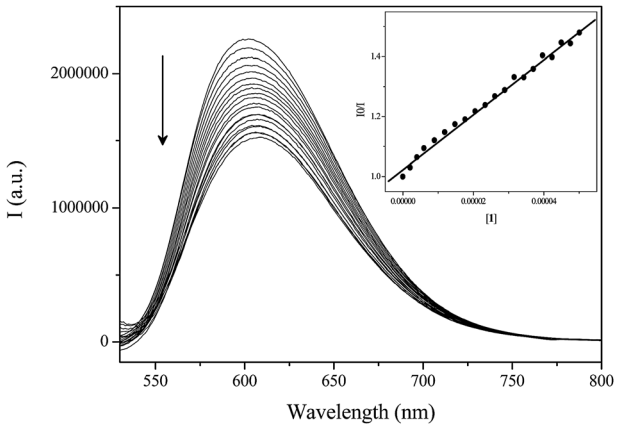

Fig. 4 Emission spectra of ethidium bromide (EB) bound to DNA in the absence and presence of increasing amounts of **1**. Inset: Stern–Volmer plot: I_0/I *vs.* [**1**].

The observed quenching of DNA–EB in the presence of **1** and **2** is shown in Fig. 4 and Fig. S4 (ESI†) and follows the Stern–Volmer equation:

$$\frac{I_0}{I} = 1 + K_q[\mathrm{Q}]$$

where I_0 and I represent the emission intensity in the absence and presence of a quencher, respectively, K_q is a linear Stern–Volmer quenching constant and [Q] is the quencher concentration, *i.e.* the concentration of the zinc–salophen derivatives in our study. This equation is considered for a static quenching, since this is the expected process for the displacement of EB by the salophen complexes. Hence, the obtained I_0/I *vs.* [Q] plots follow a linear pattern that let us to calculate K_q that is 9.4×10^3 M^{-1} and 8.1×10^3 M^{-1} for **1** and **2** respectively. Accordingly, the competitive process is favorable in a similar way for both complexes.

The different values obtained for K_b and K_q are due to the different chemical processes under study. In the UV-vis spectroscopic titrations we can calculate association constants between the compounds and DNA, while spectrofluorimetric titrations let us to calculate the quenching constant from the EB displacement process. The K_b constant could be also calculated by the luminescence quenching experiments using the representation $\log[(I_0 - I)/I]$ *vs.* log[Q] where apparent binding constants 1.8×10^3 M^{-1} and 1.6×10^3 M^{-1} could be calculated for **1** and **2** respectively. Thus, the particular process under study gives an apparent constant value, $K_{app} = K_{ass}/K_{BE}[\mathrm{EB}]$. Taking into consideration that K_{EB} is 1×10^7 M^{-1}, the

corresponding K_b values obtained from luminescence experiments are *ca.* $4.1 \times 10^5\ M^{-1}$ for both **1** and **2**, which fit quite well with those previously calculated by absorption experiments.

3.3. pH dependence stability of the complexes

Absorption spectra in DMSO/buffer solutions of **1** and **2** have been recorded in the pH range 6–9, corresponding to pH values that may be found in cellular media. The complexes are stable within this range since no significant changes are observed in UV-vis spectra. Compounds decompose at lower pH values (pH = 2 and 5) (see Fig. S5 and S6, ESI†).

3.4. Cytotoxicity studies

Evaluation of the toxicity of the compounds was necessary previously to start the study of the *in vitro* internalization on 3T3 cells and interactions of the complexes with DNA in assays.

Cytotoxicity was evaluated by MTT experiments following preparation detailed in Experimental Section. Seeded cell wells without MTT were used as blank experiments to evaluate the effect (cell binding) of **1** and **2** on the 3T3 cells. After 24 h of incubation, the cells were analyzed by fluorescence microscopy, using a UV2A filter. The best concentration of Zn complexes that seemed to interact with cells (not covering them on the outside) was *ca.* 70 μM (67.4 μM for **1** and 60.8 μM for **2**). The cytotoxic effect is exemplified in Fig. 5, where a decrease in the number of cells is observed with higher concentrations of compound **2**.

Most likely, above 70 μM concentration, the cytotoxicity does not originate exclusively from the interaction between the metal-containing compounds and the DNA, but from the excess of **1** and **2** that covers the cells (outside the cell membrane, see Fig. S7, ESI†) and does not allow proper growth.

Cytotoxicity has been evaluated with respect to the solvent control using SDS as a positive control (with a growth-inhibition value above 90%). A very large amount of the salophen derivatives (>500 μM) is required to induce cell death as shown in the dose–response curves depicted in Fig. 6.

Considering that for concentrations higher than 70 μM the compounds do not seem to interact with DNA, the growth-inhibition effects observed may be due to the cell-recovery effect by the compounds and not to the interaction with organelles and/or DNA. The growth-inhibition percentages obtained at different concentrations allowed the calculation of the 24 h IC_{50} values using a Probit regression method (that is the quantile function, *i.e.*, the inverse cumulative distribution function (CDF), associated with the standard normal distribution) included in the SPSS (Statistical Package for the Social Sciences) program version 15 for Windows (see Fig. 7 and Table 1).

Similar studies were carried out with the free ligands **L1** and **L2**. The obtained IC_{50} values after 24 h, 1.21 [461.588, 1.687] mM and 1.38 [1.21, 1.595] mM, respectively, are comparable to those of the corresponding Zn-complexes. Moreover, L1 and L2 are not luminescent and they hydrolyze rapidly in solution.

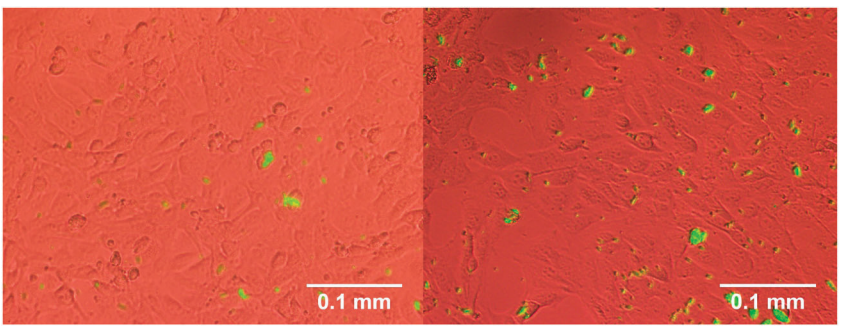

Fig. 5 Microscopy images of 3T3 fibroblast cells incubated for 24 h with 15 μM (left) and 60.8 μM of compound **2** (right). White light is used for co-localized cells. Pink tint represents culture medium; green area represents fluorescent compound **2**.

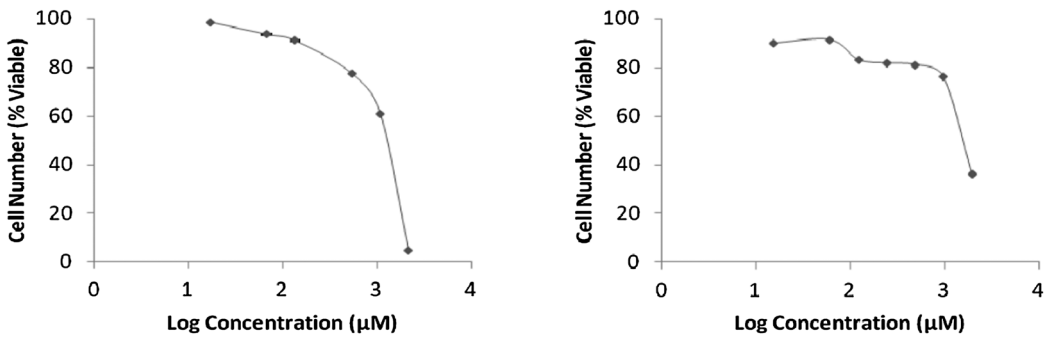

Fig. 6 Cytotoxicity dose responses of metal complexes in 3T3 cells for compound **1** (left) and **2** (right).

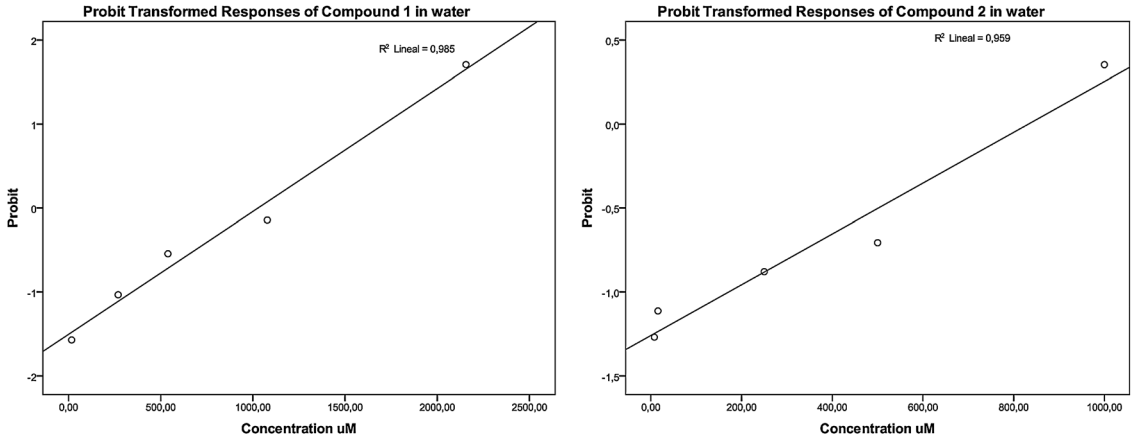

Fig. 7 Probit plot for compounds **1** and **2** at different concentrations in water and DMSO. Interception of two axes corresponds to IC_{50}.

Table 1 IC_{50} values of **1** and **2** in water. LB: lower bound. UB: upper bound

Compound	IC_{50} (mM)	[LB, UB]
1	1.29	[0.953, 1.453]
2	1.85	[1.214, 2.456]

The potential cytotoxic properties of the zinc compounds and ligands were also examined at a longer incubation time (72 h) but no significant changes were noticed.

3.5. Genotoxicity: comet assays

Comet assays, as genotoxicity experiments, were carried out with 3T3 fibroblast cells to investigate whether our zinc compounds interact with the DNA strands (a polyphosphate macromolecule that may indeed bind **1** and/or **2**) and produce damages. This well-established and extremely sensitive method is commonly applied to detect DNA fragmentation in individual cells, thus allowing the assessment of genotoxic effects, or the anti-genotoxic (protective) activity against a clastogenic challenge (*i.e.* chromosome breakage[71]).

Non-damaged cells exhibit a spherical shape, while fragmented nucleoids migrate, forming a tail (''comet'' shape). The nucleoid damage was quantified as fluorescence percentage in the tail. Comparison of the results with a positive control (methyl methanesulfonate, MMS) reveals that the nucleoid is not damaged by the two zinc–salophen complexes (see Fig. 8 and Fig. S7, ESI†).

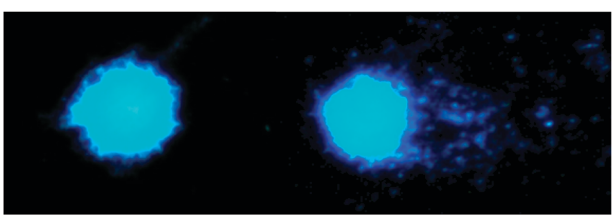

Fig. 8 40× microscopy image of cells in DAPI-staining solution, using a UV2A fluorescence filter. Image of the cells in the presence of compound **2** (left) and in the presence of the MMS positive control (right).

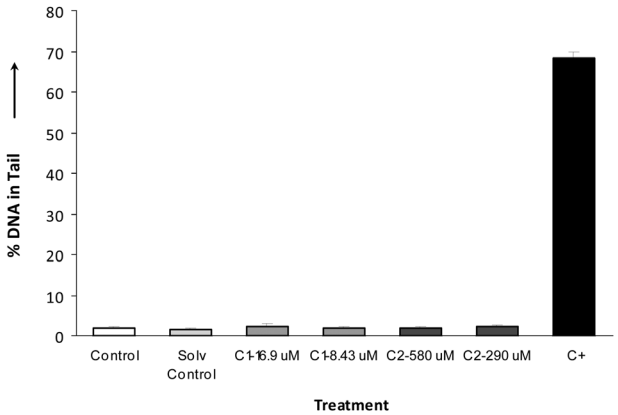

Fig. 9 Histogram of the genotoxicity assay results for compounds **1** and **2** with 3T3 cells. Control: culture medium; solvent control 10% water; C1: compound **1**; C2: compound **2**; C+: positive control (MMS).

As shown in Fig. 9, the genotoxicity of the salophen derivatives is clearly lower than that observed for the MMS control. This feature is consistent with a lack of DNA (nucleoid)-damage activity in cells.

3.6. Preliminary cellular uptake studies

First of all, cellular uptake studies were therefore carried out using 3T3 fibroblasts (connective tissue cells). After incubation with compound **1** or **2**, the cultures were washed and the cells were observed under an inverted fluorescence microscope with an ultraviolet filter. Interestingly, as it is evidenced in Fig. 10, fluorescence is observed for cells incubated with the two compounds, suggesting that both **1** and **2** can interact with cells.

The optimal time required for the cell uptake/binding was analyzed by taking pictures at 5 min, 30 min, 1 h, 1.5 h, 2 h and 2.5 h. The corresponding microscopy images indicate that the binding of the compounds appears optimal after an incubation time of about 1 h. Above 1 h, **1** and **2** are uptaken by the cells, but their binding effect does not seem to increase significantly (see Fig. S8 and S9, ESI†). The strong fluorescence observed at

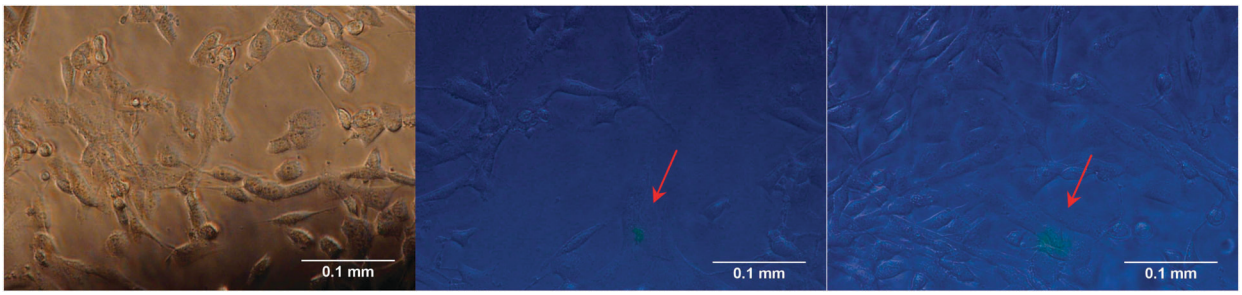

Fig. 10 Microscopy image of 3T3 fibroblast cells with white light for localized cells (left), fluorescent image of 3T3 fibroblast cells incubated with **1** (70 μM), 20× and UV2A filter (middle) and 3T3 fibroblast cells incubated with **2** (70 μM), 20× and UV2A filter (right). Incubation time: 1 h.

incubation times of 1.5 h, 2 h and 2.5 h most likely arises from an excess of the fluorophores covering the cells, namely located outside the cellular membrane.

3.7. DNA binding and interaction within the cells

After a quick exposure to compounds **1**, **2** (107.78, 97.29 μM concentrations respectively) over fixed nucleoids, it is possible to see how the compounds interact with DNA in a specific region (see Fig. 11, right and Fig. S11, right, ESI†). DAPI stains cell nuclei blue as a result of its emission at 461 nm (when excited at 358 nm); hence, this technique is routinely used to visualize nuclear morphologies. Usually, more intensely DAPI-stained regions indicate more condensed DNA and *vice versa*.[72]

The presence of Zn(II)–salophen complexes seems to be detected in the cell nucleus (yellow-green dots in Fig. 11, left). Moreover, the DAPI-staining experiments and genotoxicity assay suggest that the metal-coordination compound could be located inside the nucleus, without affecting its integrity (Fig. 11, right). Well-defined nucleoids are observed, *i.e.* the internalization appears to occur without damaging the nucleus (*in vitro* studies).

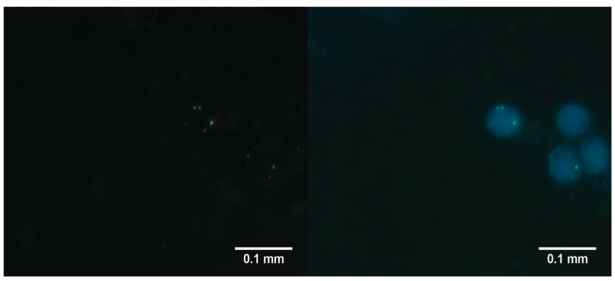

Fig. 11 20× Fluorescence microscopy image of nucleoids incubated with compound **2** (concentration of 97.29 μM) and in the presence of DAPI. Left: with a B2A filter without DAPI co-staining (see the staining of compound **2**); right: with a UV2A filter (see the staining of DAPI). Incubation time: 1 h.

However, analysis of the same samples after 3 days reveals an inhibiting effect on cell growth in the presence of compounds **1** and **2**. Therefore, the interaction of the zinc derivatives with the DNA strands appears to prevent cell division. It should be noticed as well that the compounds seem to bind at specific DNA sites. Hence, the DNA/compound interaction is not uniform (see Fig. 11 and Fig. S11, ESI†) and appears to be present in different organelles (not only in the nucleoid). To analyze further these data, co-localization of living cell internalization was investigated by using Draq5 as fluorochrom. This is a far-red emitting fluorescent DNA dye used for permeabilized and fixed live cell analysis that can be used in combination with other common fluorophores. In the present case, the utilization of Draq5 proved to be appropriate since its red emission could be clearly separated from that of the zinc–salophen derivatives (observed at higher energies). Thus, 3T3 cells were stained with Draq5 and the emissions were observed by a fluorescence confocal microscope at 688 nm for Draq5 and at 500 nm for the complexes. Lambda scans from 405 nm to 600 nm were performed.

The corresponding images displayed in Fig. 12 and Fig. S12 (ESI†) clearly show that the nucleus is stained by Draq5 (Fig. 12, left), and that the zinc complexes seem to enter the cells (Fig. 12, middle), but without binding specifically to the nucleus. Superimposition of the images (see Fig. 12, right) indeed indicates that the red staining due to Draq5 is not mixed with that corresponding to the salophen compounds.

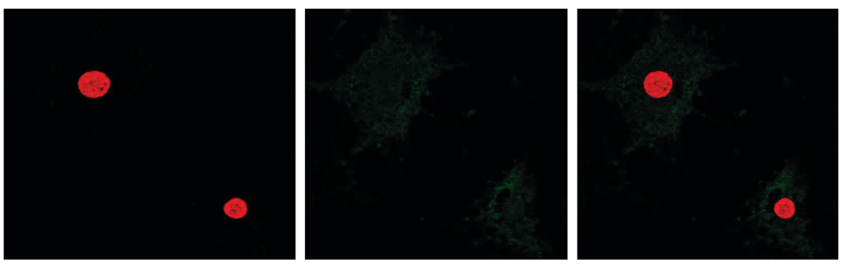

Fig. 12 Fluorescence confocal microscopy image of 3T3 incubated cells with Draq5 (red color stain nucleus DNA, left), salophen complex **1** (concentration of 107.78 μM green color, middle) and superimposed images (right). Incubation time: 3 h.

Accordingly, these first co-localization experiments demonstrate that although the zinc–salophen complexes **1** and **2** enter the living cells, they do not enter the nucleus, since no mixture of colours could be observed in the nucleus region. This is perfectly in agreement with the lack of nucleoid damage previously observed with the *in vivo* comet assay.

4. Conclusions

Two luminescent zinc–salophen compounds, **1** and **2**, have been assessed as potential DNA-intercalator agents with the prospective of using them as bio-markers for cell imaging. AFM studies together with emission and UV-vis titration experiments with ethidium bromide are indicative of interaction with DNA. Cell-growth inhibition investigations are also in agreement with *in vitro* studies. Actually, both compounds can enter the cells and remain inside. Comet assays clearly show that this cellular uptake does not lead to nucleoid damage. The observed interaction of the complexes with DNA *in vitro* encouraged us to investigate their activity in a living biological system. Staining experiments with Draq5 on 3T3 fibroplast cells have indeed demonstrated that the compounds enter the cells but do not reach the nucleus. These features, together with the very high IC_{50} 24 hours values obtained for **1** and **2**, indicate their non-cytotoxic character and encourage their use as fluorescence markers in cells. Their high energy emission properties would allow them to be easily followed by two-photon microscopy imaging. To complete the investigation, the cytotoxicity of the metal-free ligands **L1** and **L2** has been evaluated in a similar way. The obtained IC_{50} values are comparable to those of the corresponding Zn-complexes, but their lack of luminescence and low stability precludes their use as fluorescence markers.

Acknowledgements

The support and sponsorship provided by COST Action CM1005 are acknowledged. Authors are also grateful to the Ministerio de Ciencia e Innovación of Spain (Projects Project CTQ2012-31335 and CTQ2011-27929-C02-01) and Fundação para a Ciência e Tecnologia of Portugal (PTDC/QUI-QUI/112597/2009). Authors would like to thank Drs Lidia Bardia and Julien Collombelli from IRB-Barcelona for fruitful discussions.

References

1 X. Michalet, F. F. Pinaud, L. A. Bentolila, J. M. Tsay, S. Doose, J. J. Li, G. Sundaresan, A. M. Wu, S. S. Gambhir and S. Weiss, *Science*, 2005, **307**, 538.
2 V. Fernandez-Moreira, F. L. Thorp-Greenwood and M. P. Coogan, *Chem. Commun.*, 2010, **46**, 186.
3 H. Kobayashi, M. R. Longmire, M. Ogawa and P. L. Choyke, *Chem. Soc. Rev.*, 2011, **40**, 4626.
4 D. A. Mankoff, *J. Nucl. Med.*, 2007, **48**, 18N.
5 R. D. Goldman, J. R. Swedlow and D. L. Spector, *Live Cell Imaging*, Cold Spring Harbor Laboratory Press, New York, 2010.
6 J. R. Lakowicz, *Principles of Fluorescence Spectroscopy*, Plenum, New York, 2nd edn, 1999.
7 S. W. Hell, *Science*, 2007, **316**, 1153.
8 M. J. Rust, M. Bates and X. Zhuang, *Nat. Methods*, 2006, **3**, 793.
9 J. Jaiswal and S. M. Simon, *Nat. Chem. Biol.*, 2007, **3**, 92.
10 X. S. Xie, J. Yu and W. Y. Yang, *Science*, 2006, **312**, 228.
11 D. J. Stephens and V. J. Allan, *Science*, 2003, **300**, 82.
12 G. U. Nienhaus and J. Wiedenmann, *ChemPhysChem*, 2009, **10**, 1369.
13 L. Kurzawa and M. C. Morris, *ChemBioChem*, 2010, **11**, 1037.
14 A. Paganin-Gioanni, E. Bellard, L. Paquereau, V. Ecochard, M. Golzio and J. Teissié, *Radiol. Oncol.*, 2010, **44**, 142.
15 H. Hong, S. Goel, Y. Zhang and W. Cai, *Curr. Med. Chem.*, 2011, **18**, 4195.
16 F. Wang, W. B. Tan, Y. Zhang, X. Fan and M. Wang, *Nanotechnology*, 2006, **17**, R1.
17 J. A. Drewry and P. T. Gunning, *Coord. Chem. Rev.*, 2011, **255**, 459.
18 R. M. Haak, S. J. Wezenberg and A. W. Kleij, *Chem. Commun.*, 2010, **46**, 2713.
19 B. Bahramian, V. Mirkhani, M. Moghadam and A. H. Amin, *Appl. Catal., A*, 2006, **315**, 52.
20 N. S. Venkataramanan, G. Kuppuraj and S. Rajagopal, *Coord. Chem. Rev.*, 2005, **249**, 1249.
21 K. Omura, T. Uchida, R. Irie and R. Katsuki, *Chem. Commun.*, 2004, 2060.
22 J. D. McGilvra and V. H. Rawal, *Synlett*, 2004, 2440.
23 A. Dalla Cort, L. Mandolini and L. Schiaffino, *Chem. Commun.*, 2005, 3867.
24 C. K. Shin, S. J. Kim and G. J. Kim, *Tetrahedron Lett.*, 2004, **45**, 7429.
25 T. Maeda, T. Takeuchi, Y. Furusho and T. J. Takata, *J. Polym. Sci., Part A: Polym. Chem.*, 2004, **42**, 4693.
26 S. S. Kim and G. Rajagopal, *Synthesis*, 2003, 2461.
27 J. L. Czlapinski and T. L. Sheppard, *J. Am. Chem. Soc.*, 2001, **123**, 8618.
28 S. Bhattacharya and S. S. Mandal, *Chem. Commun.*, 1996, 1515.
29 J. G. Muller, S. J. Paikoff, S. E. Rokita and C. J. Burrows, *J. Inorg. Biochem.*, 1994, **54**, 199.
30 S. Routier, J. L. Bernier, M. J. Waring, P. Colson, C. Houssier and C. Bailly, *J. Org. Chem.*, 1996, **61**, 2326.
31 D. J. Gravert and J. H. Griffin, *J. Org. Chem.*, 1993, **58**, 820.
32 H. Y. Shrivastava, S. N. Devaraj and B. U. Nair, *J. Inorg. Biochem.*, 2004, **98**, 387.
33 A. Dalla Cort, P. De Bernadin, G. Forte and F. Yafteh Mihan, *Chem. Soc. Rev.*, 2010, **39**, 3863.
34 K. I. Ansari, S. Kasiri, J. D. Grant and S. S. Mandal, *Dalton Trans.*, 2009, 8525.
35 A. Hille, I. Ott, A. Kitanovic, I. Kitanovic, H. Alborzinia, E. Lederer, S. Wölfl, N. Metzler-Nolte, S. Schäfer, W. S. Sheldrick, C. Bischof, U. Schatzschneider and R. Gust, *J. Biol. Inorg. Chem.*, 2009, **14**, 711.
36 S. Routier, H. Vezin, E. Lamour, J. L. Bernier, J. P. Catteau and C. Bailly, *Nucleic Acids Res.*, 1999, **27**, 4160.

37 T. S. Lange, K. K. Kim, R. K. Singh, R. M. Strongin, C. K. McCourt and L. Brard, *PLoS One*, 2008, **3**, e2303, 1.
38 Y. W. Liou and C. M. Wang, *J. Electroanal. Chem.*, 2000, **481**, 102.
39 J. G. Muller, L. A. Kayer, S. J. Paikoff, V. Duarte, N. Tang, R. J. Pérez, S. E. Rokita and C. J. Burrows, *Coord. Chem. Rev.*, 1999, **185–186**, 761.
40 O. Alptürk, O. Rusin, S. O. Fakayode, W. Wang, J. O. Escobedo, I. M. Warner, W. E. Crowe, V. Král, J. M. Pruet and R. M. Strongin, *Proc. Natl. Acad. Sci. U. S. A.*, 2006, **103**, 9756.
41 S. R. Doctrow, K. Huffman, C. B. Marcus, G. Tocco, E. Malfroy, C. A. Adinolfi, H. Kruk, K. Baker, N. Lazarowych, J. Mascarenhas and B. Malfroy, *J. Med. Chem.*, 2002, **45**, 4549.
42 Y. Rong, S. R. Doctrow, G. Tocco and M. Baudry, *Proc. Natl. Acad. Sci. U. S. A.*, 1999, **96**, 9897.
43 R. Chico, C. Domínguez, B. Donnio, S. Coco and P. Espinet, *Dalton Trans.*, 2011, **40**, 5977.
44 L. Zhou, P. Cai, Y. Feng, J. Cheng, H. Xiang, J. Liu, D. Wu and X. Zhou, *Anal. Chim. Acta*, 2012, **735**, 96.
45 S. Di Bella, I. P. Oliveri, A. Colombo, C. Dragonetti, S. Righetto and D. Roberto, *Dalton Trans.*, 2012, **41**, 7013.
46 J. E. Reed, A. Arola Arnal, S. Neidle and R. Vilar, *J. Am. Chem. Soc.*, 2006, **128**, 5992.
47 A. Arola-Arnal, J. Benet-Buchholz, S. Neidle and R. Vilar, *Inorg. Chem.*, 2008, **47**, 11910.
48 N. H. Campbell, N. H. Abd Karim, G. N. Parkinson, M. Gunaratnam, V. Petrucci, A. K. Todd, R. Vilar and S. Neidle, *J. Med. Chem.*, 2012, **55**, 209.
49 P. Wu, D.-L. Ma, C.-H. Leung, S.-C. Yan, N. Zhu, R. Abagyan and C.-M. Che, *Chem.–Eur. J.*, 2009, **15**, 13008.
50 S. I. Pascu, P. A. Waghorn, T. D. Conry, B. Lin, H. M. Betts, J. R. Dilworth, R. B. Sim, G. C. Churchill, F. I. Aigbirhio and J. E. Warren, *Dalton Trans.*, 2008, 2107.
51 A. L. Singer and D. A. Atwood, *Inorg. Chim. Acta*, 1998, **277**, 157.
52 Y. Hai, J.-J. Chen, P. Zhao, H. Lv, Y. Yu, P. Xu and J.-L. Zhang, *Chem. Commun.*, 2011, **47**, 2435.
53 Y. Gao, J. Wu, Y. Li, P. Sun, H. Zhou, J. Yang, S. Zhang, B. Jin and Y. Tian, *J. Am. Chem. Soc.*, 2009, **131**, 5208.
54 M. E. Germain, T. R. Vargo, B. A. McClure, J. J. Rack, P. G. Van Patten, M. Odoi and M. J. Knapp, *Inorg. Chem.*, 2008, **47**, 6203.
55 A. Dalla Cort, L. Mandolini, C. Pasquini, K. Rissanen, L. Russo and L. Schiaffino, *New J. Chem.*, 2007, **31**, 1633.
56 M. Cano, L. Rodríguez, J. C. Lima, F. Pina, A. Dalla Cort, C. Pasquini and L. Schiaffino, *Inorg. Chem.*, 2009, **48**, 6229.
57 S. J. Wezenberg, E. C. Escudero-Adán, J. Benet-Buchholz and A. W. Kleij, *Chem.–Eur. J.*, 2009, **15**, 5695.
58 A. Dalla Cort, P. De Bernardin and L. Schiaffino, *Chirality*, 2009, **21**, 104.
59 I. P. Oliveri and S. Di Bella, *Tetrahedron*, 2011, **67**, 9446.
60 G. Consiglio, S. Failla, P. Finocchiaro, I. P. Oliveri and S. Di Bella, *Dalton Trans.*, 2012, **41**, 387.
61 I. P. Oliveri, G. Maccarrone and S. Di Bella, *J. Org. Chem.*, 2011, **76**, 8879.
62 G. Consiglio, S. Failla, I. P. Oliveri, R. Purrello and S. Di Bella, *Dalton Trans.*, 2009, 10426.
63 J. Jing, J. J. Chen, Y. Hai, J. Zhan, P. Xu and J.-L. Zhang, *Chem. Sci.*, 2012, **3**, 3315.
64 E. Verner, B. A. Katz, J. R. Spencer, D. Allen, J. Hataye, W. Hruzewicz, H. C. Hui, A. Kolesnikov, Y. Li, C. Luong, A. Martelli, K. Radika, R. Rai, M. She, W. Shrader, P. A. Sprengeler, S. Trapp, J. Wang, W. B. Young and R. L. Mackman, *J. Med. Chem.*, 2001, **44**, 2753.
65 ASTM-E2186, *Standard Guide for Determining DNA Single-Strand Damage in Eukaryotic Cells using the Comet Assay*, June 2003.
66 H. Wang, R. Shen, J. Wu and N. Tang, *Chem. Pharm. Bull.*, 2009, **57**, 814.
67 A. Wolfe, G. H. Shimer Jr and T. Meehan, *Biochemistry*, 1987, **26**, 6392.
68 P. Krishnamoorthy, P. Sathyadevi, A. H. Cowley, R. R. Butorac and N. Dharmaraj, *Eur. J. Med. Chem.*, 2011, **46**, 3376.
69 M. Shilpa, P. Nagababu, Y. P. Kumar, J. N. Lavanya Latha, M. R. Reddy, K. S. Karthikeyan, N. Md. Gabra and S. Satyanarayana, *J. Fluoresc.*, 2011, **21**, 1155.
70 S. J. Lippard, *Acc. Chem. Res.*, 1978, **11**, 211.
71 M. Barenys, N. Macia, L. Camps, J. de Lapuente, J. Gómez-Catalan, J. González-Linares, M. Borràs, M. Rodamilans and J. M. Llobet, *Toxicol. Lett.*, 2009, **191**, 40.
72 K. I. Ansari, B. P. Mishra and S. S. Mandal, *Biochim. Biophys. Acta*, 2008, **1779**, 66.